PHYSICAL REVIEW D **92,** 074038 (2015)

Chiral dynamics and S-wave contributions in semileptonic D_s/B_s decays into $\pi^+\pi^-$

Yu-Ji Shi[1,†] and Wei Wang[1,2,*]

[1]*INPAC, Shanghai Key Laboratory for Particle Physics and Cosmology, Department of Physics and Astronomy, Shanghai Jiao-Tong University, Shanghai 200240, China*

[2]*State Key Laboratory of Theoretical Physics, Institute of Theoretical Physics, Chinese Academy of Sciences, Beijing 100190, China*

(Received 30 July 2015; published 26 October 2015)

In this work, we study the semileptonic decay modes $B_s^0 \to \pi^+\pi^-\ell^+\ell^-$ and $D_s^+ \to \pi^+\pi^-\ell^+\nu$ in the kinematics region where the $\pi^+\pi^-$ system has a invariant mass in the range 0.5–1.3 GeV. These processes are valuable towards the determination of S-wave $\pi^+\pi^-$ light-cone distribution amplitudes whose normalizations are scalar form factors. We compare the results for scalar form factors predicted in unitarized chiral perturbation theory and extracted from the data on the $B_s \to J/\psi\pi^+\pi^-$. Then the $B_s \to \pi^+\pi^-$ and $D_s \to \pi^+\pi^-$ form factors are calculated in light-cone sum rules, based on which predictions for differential decay widths are made. The results are in good agreement with the experimental data on the B_s and D_s decays into $\pi^+\pi^-$. More accurate measurements at BEPC, LHC and KEKB in the future will be helpful to examine our formalism and constrain the input parameters more precisely.

DOI: 10.1103/PhysRevD.92.074038 PACS numbers: 12.39.Fe, 13.20.He

I. INTRODUCTION

It is anticipated that new physics (NP) beyond the standard model (SM) can be indirectly probed through the precision exploration of low-energy processes. An ideal platform is to study the flavor-changing neutral current (FCNC). Rare B decays like the $b \to s\ell^+\ell^-$, with tiny decay probabilities in the SM, are sensitive to NP degrees of freedom and thus can be exploited as indirect searches of these unknown effects. In terms of observables ranging from the decay probabilities, forward-backward asymmetries, polarizations to a full angular analysis, the exclusive decay mode $B \to K^*\ell^+\ell^-$ can provide us with a wealth of information on weak interactions. Recent measurements of the almost form-factor independent ratio P_5' by the LHCb Collaboration have indicated a deviation from the SM by about 3.7σ [1,2].

In fact, the $B \to K^*\ell^+\ell^-$ is a four-body decay process since the K^* meson is reconstructed in the $K\pi$ final state. Thus it is more appropriate to explore the $B \to M_1M_2\ell^+\ell^-$, in which various partial-waves of M_1M_2 contribute [3–5]. The S-wave contributions to $B \to K\pi\ell^+\ell^-$ have been discussed for instance in Refs. [6–12]. The bottom mass m_b is much heavier than the hadronic scale $\Lambda_{\rm QCD}$, which allows an expansion of the hard-scattering kernels in terms of the strong coupling constant α_s and the power-scaling parameter $\Lambda_{\rm QCD}/m_b$. On the other side, final state interactions among the two-light hadrons should be constrained by unitarity and analyticity. A formalism that makes use of these two advantages has been developed in Refs. [12–14], and summarized in Ref. [15]. Such an approach was pioneered in Ref. [16,17], and a method without the analysis of hard-scattering kernels has been explored recently in Refs. [18–24]. See also Refs. [25–28] for attempts to analyze charmless three-body B decays. The aim of this work is to further examine this formalism by confronting the theoretical results with the relevant data on $B_s \to \pi^+\pi^-\mu^+\mu^-$ and $D_s \to \pi^+\pi^-e^+\nu_e$.

On the theoretical side, the S-wave $\pi^+\pi^-$ state has the same quantum number $J^{\rm PC} = 0^{++}$ with QCD vacuum, and thus the dynamics is very complex. In particular, quite a few scalar resonances exist, for example $f_0(600)$ and $f_0(980)$ below 1 GeV, and $f_0(1370)$, $f_0(1500)$ and $f_0(1710)$ above 1 GeV. For a few decades, the internal structure of these scalar mesons is controversial since the $\bar{q}q$ component can get entangled with the tetraquark configuration, scalar glueball, and a hadronic molecule [29–33]. Heavy mesons like the B and D must decay via weak interaction, and consequently the quark structure in the final state is less ambiguous in these decays. Moreover due to the large bottom quark mass, factorization may be established in certain B decays which will greatly simplify the dynamics. Thus it has been proposed that the semileptonic and nonleptonic decays of heavy mesons are of great values to probe the internal structure of scalar resonances [34–60]. The large amount of data accumulated by various experimental facilities, mostly B factories and the LHC experiment, gradually make this proposal become a reality.

On the experimental side, the LHCb Collaboration has systematically investigated the $B_s \to J/\psi\pi^+\pi^-$ decays [61–68] (see also measurements by Belle [69], CDF [70] and D0 [71]), and some implications on the structure of

*Corresponding author.
wei.wang@sjtu.edu.cn
†shiyuji@sjtu.edu.cn

scalar mesons have been explored in Refs. [20,72]. Recently, the LHCb Collaboration has performed an analysis of rare B_s decays into the $\pi^+\pi^-\mu^+\mu^-$ final state with the measured branching ratio [73],

$$\mathcal{B}(B_s \to \pi^+\pi^-\mu^+\mu^-) = (8.6 \pm 1.5 \pm 0.7 \pm 0.7) \times 10^{-8}, \tag{1}$$

where the errors are statistical, systematic and arise from the normalization, respectively. The dominant contribution is the $B_s \to f_0(980)\mu^+\mu^-$ [73]:

$$\mathcal{B}(B_s \to f_0(980)(\to \pi^+\pi^-)\mu^+\mu^-) = (8.3 \pm 1.7) \times 10^{-8}. \tag{2}$$

This has triggered theoretical interpretations based on two-meson light-cone distribution amplitudes (LCDAs) [74,75].

Previously, the CLEO Collaboration investigated the $D_s \to \pi^+\pi^-\ell\nu_e$, in which the $f_0(980)$ contribution is found dominant as well [76,77]

$$\mathcal{B}(D_s \to f_0(980)(\to \pi^+\pi^-)e^+\nu_e) = (2.0 \pm 0.3 \pm 0.1) \times 10^{-3}. \tag{3}$$

A recent analysis based on the CLEO-c data [78] gives a similar result

$$\mathcal{B}(D_s \to f_0(980)(\to \pi^+\pi^-)e^+\nu_e) = (1.3 \pm 0.2 \pm 0.1) \times 10^{-3}. \tag{4}$$

The BES-III Collaboration will collect about 2 fb^{-1} data in e^+e^- collision at the energy around 4.17 GeV, which will be used to study semileptonic and nonleptonic D_s decays [79].

The rest of this paper is organized as follows. In Sec. II, we will give the results for scalar $\pi\pi$ form factors and the nonlocal LCDAs. Section III will be devoted to the calculation of the $B_s \to \pi^+\pi^-$ and $D_s \to \pi^+\pi^-$ form factors in the light-cone sum rules (LCSR) at leading order. In Sec. IV, phenomenological results for a variety of observables in the $B_s \to \pi^+\pi^-\ell^+\ell^-$, $B_s \to \pi^+\pi^-\nu\bar{\nu}$ and $D_s \to \pi^+\pi^-\ell\nu$ are presented, and compared to the experimental data if available. An agreement between theory and data will be shown in this section. Our conclusions will be given in Sec. V.

II. SCALAR $\pi^+\pi^-$ FORM FACTORS AND S-WAVE LCDAS

A. Scalar form factor

We start with the definition of a scalar form factor:

$$\langle \pi^+\pi^-|\bar{s}s|0\rangle = B_0 F^s_{\pi\pi}(m^2_{\pi\pi}), \tag{5}$$

and the B_0 is the QCD condensate parameter:

$$\langle 0|\bar{q}q|0\rangle \equiv -f_\pi^2 B_0, \tag{6}$$

with f_π as the leading order (LO) pion decay constant. For the numerics, we use $f_\pi = 91.4$ MeV and $\langle 0|\bar{q}q|0\rangle = -[(0.24 \pm 0.01)\,\text{GeV}]^3$ [80]. This corresponds to $B_0 = (1.7 \pm 0.2)\,\text{GeV}$.

In the literature, a variety of theoretical methods have been adopted to calculate the $F^s_{\pi\pi}(m^2_{\pi\pi})$, including the (unitarized) chiral perturbation theory (χPT) [81–88] and dispersion relations [89]. In the χPT, the LO and next-to-leading order (NLO) results can be obtained by computing the Feynman diagrams in Fig. 1. These results can describe the low-energy data with good accuracy [81–88].

Since the perturbative expansion in χPT is organized in terms of $p_\pi/(4\pi f_\pi)$, the χPT becomes invalid when the pion momentum p_π gets very large. It has been suggested that higher order corrections can be summed in an approximate way, and this approach is referred to as the unitarized approach [90,91]. A sketch of the summation scheme, in particular the s-channel process, is shown in Fig. 2. As an example, the scalar form factor can be expressed in terms of the algebraic coupled-channel equation

$$F(s) = R(s)[I + g(s)K(s)]^{-1}, \tag{7}$$

where the $g(s)$ and $K(s)$ denotes the loop function and the scattering amplitude, respectively. The remanent $R(s)$ can be obtained by matching the above equation to the NLO results in χPT. Their explicit expressions can be found in Refs. [82,84].

As a phenomenological method, the unitarized approach can extend the applicability of χPT to the scale around 1 GeV [90–94] and is able to describe the relevant low-energy data. For instance, a fit of the unitarized χPT to the BES data on the $\pi\pi$ invariant mass distributions

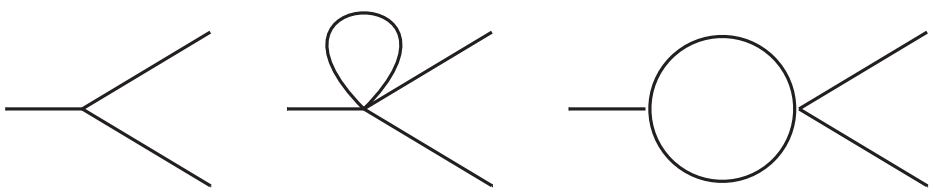

FIG. 1. Feynman diagrams for the scalar form factor at tree level and one-loop level in χPT. The wave function renormalization diagrams are not shown here.

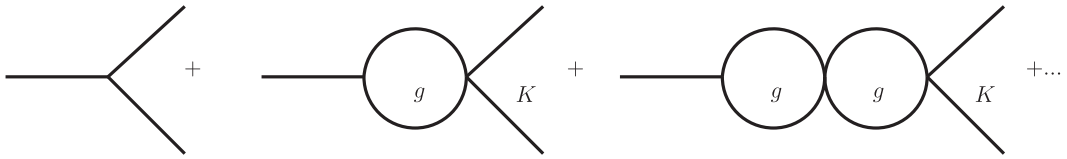

FIG. 2. The s-channel diagrams to the scalar $\pi\pi$ form factors in χPT. With the increase of the $\pi\pi$ invariant mass, higher-order contributions may become important. In the unitarized approach [90], these diagrams can be summed, which can extend the applicability up to 1 GeV.

in $J/\psi \to \pi^+\pi^-\phi$ [95] has been performed in this approach and an overall agreement is found [82,84]. The fitted result for $F^s_{\pi\pi}(m^2_{\pi\pi})$ is shown in Fig. 3, and we refer the reader to Refs. [82,84] for more details. The modulus, real part and imaginary part are shown as solid, dashed and dotted curves, from which one can observe the broad structure for the $\sigma(600)$ and the peak at $f_0(980)$ is naturally produced.

In recent years the LHCb Collaboration has conducted a series of analyses of angular distributions in the $B_s \to J/\psi\pi^+\pi^-$ decay mode [66,67]. In this procedure, the S-wave contributions have been explicitly separated, and three resonances, $f_0(980)$, $f_0(1500)$ and $f_0(1790)$, have been identified. To access the $\pi^+\pi^-$ invariant mass distribution, the Breit-Wigner formula is employed for the $f_0(1500)$ and $f_0(1790)$. Due to the fact that the $f_0(980)$ lies in the vicinity of the $K\bar{K}$ threshold, the Flatté model [96,97] has been adopted. Considering the relative strengths and strong phases among different resonances, we have

$$F^s_{\pi\pi}(m^2_{\pi\pi}) = \frac{c_1 m^2_{f_0(980)} e^{i\theta_1}}{m^2_{\pi\pi} - m^2_{f_0(980)} + i m_{f_0(980)}(g_{\pi\pi}\rho_{\pi\pi} + g_{KK}F^2_{KK}\rho_{KK})} + \frac{c_2 m^2_{f_0(1500)} e^{i\theta_2}}{m^2_{\pi\pi} - m^2_{f_0(1500)} + i m_{f_0(1500)}\Gamma_{f_0(1500)}(m^2_{\pi\pi})} + \frac{c_3 m^2_{f_0(1790)} e^{i\theta_3}}{m^2_{\pi\pi} - m^2_{f_0(1790)} + i m_{f_0(1790)}\Gamma_{f_0(1790)}(m^2_{\pi\pi})}. \quad (8)$$

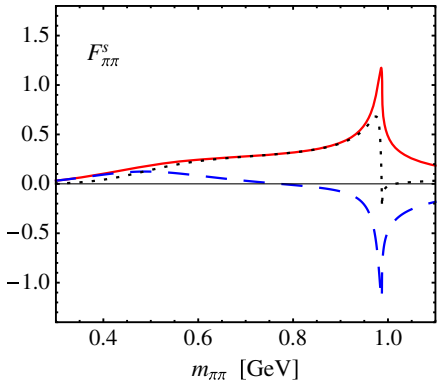

FIG. 3 (color online). The $F^s_{\pi\pi}(m^2_{\pi\pi})$ in unitarized χPT. The modulus, real part and imaginary part are shown in solid, dashed and dotted curves. The result is based on the fit of the BES data on the $\pi\pi$ invariant mass distributions in $J/\psi \to \pi^+\pi^-\phi$ [95] in Ref. [84].

The $\rho_{\pi\pi}$ and ρ_{KK} are phase space factors [66,67,97]:

$$\rho_{\pi\pi} = \frac{2}{3}\sqrt{1 - \frac{4m^2_{\pi^\pm}}{m^2_{\pi\pi}}} + \frac{1}{3}\sqrt{1 - \frac{4m^2_{\pi^0}}{m^2_{\pi\pi}}},$$
$$\rho_{KK} = \frac{1}{2}\sqrt{1 - \frac{4m^2_{K^\pm}}{m^2_{\pi\pi}}} + \frac{1}{2}\sqrt{1 - \frac{4m^2_{K^0}}{m^2_{\pi\pi}}}. \quad (9)$$

Compared to the normal Flatté distribution, an additional correction has been introduced in the LHCb fit above the $K\bar{K}$ threshold to better describe the data [67]

$$F_{KK} = \exp(-\alpha k^2), \quad (10)$$

where k is the kaon momentum in the $K\bar{K}$ rest frame, and α is set to $\alpha = 2.0\ \text{GeV}^{-2}$ [67]. The energy-dependent width $\Gamma_S(m^2_{\pi\pi})$ for an S-wave resonance is parametrized as

$$\Gamma_S(m^2_{\pi\pi}) = \Gamma_S \frac{m_S}{m_{\pi\pi}} \left(\frac{m^2_{\pi\pi} - 4m^2_\pi}{m^2_S - 4m^2_\pi}\right)^{\frac{1}{2}} F^2_R, \quad (11)$$

with the constant width Γ_S, and the Blatt-Weisskopf barrier factor $F_R = 1$ [67]. The c_i and θ_i, $i = 1, 2$, and 3 are tunable

TABLE I. Fitted parameters for contributing components in the $B_s \to J/\psi\pi^+\pi^-$ by the LHCb Collaboration [67]. Two solutions are found in the fit.

Fractions (%)	Solution I	Solution II
$f_0(980)$	$70.3 \pm 1.5^{+0.4}_{-5.1}$	$92.4 \pm 2.0^{+0.8}_{-16.0}$
$f_0(1500)$	$10.1 \pm 0.8^{+1.1}_{-0.3}$	$9.1 \pm 0.9 \pm 0.3$
$f_0(1790)$	$2.4 \pm 0.4^{+5.0}_{-0.2}$	$0.9 \pm 0.3^{+2.5}_{-0.1}$
Phase differences (°)	**Solution I**	**Solution II**
$f_0(1500) - f_0(980)$	138 ± 4	177 ± 6
$f_0(1790) - f_0(980)$	78 ± 9	95 ± 16
Parameter	**Solution I**	**Solution II**
$m_{f_0(980)}$ (MeV)	945.4 ± 2.2	949.9 ± 2.1
$g_{\pi\pi}$ (MeV)	167 ± 7	167 ± 8
$g_{KK}/g_{\pi\pi}$	3.47 ± 0.12	3.05 ± 0.13
$m_{f_0(1500)}$ (MeV)	1460.9 ± 2.9	1465.9 ± 3.1
$\Gamma_{f_0(1500)}$ (MeV)	124 ± 7	115 ± 7
$m_{f_0(1790)}$ (MeV)	1814 ± 18	1809 ± 22
$\Gamma_{f_0(1790)}$ (MeV)	328 ± 34	263 ± 30

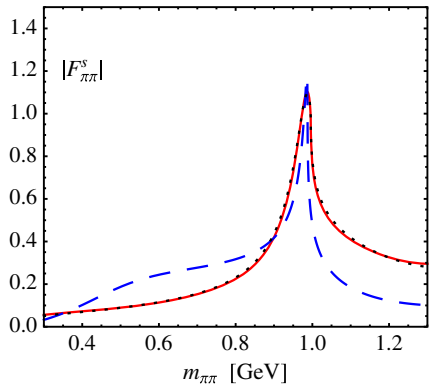

FIG. 4 (color online). The $F^s_{\pi\pi}(m^2_{\pi\pi})$ predicted in the χPT (dashed curve), and fitted from the $B_s \to J/\psi\pi^+\pi^-$ data (solid line for solution I and dotted line for solution II). The two fitted solutions are not distinguishable below 1.3 GeV. It is necessary to stress that it is not theoretically justified to apply the χPT to the region above 1 GeV.

parameters. In the fit by LHCb, two solutions are found and the fitted parameters for three contributing components are collected in Table I [67].

In Fig. 4, we compare the results for the scalar form factor calculated in the unitarized χPT (dashed curve), and the ones extracted from the $B_s \to J/\psi\pi^+\pi^-$ data based on Eq. (8) (solid and dotted curves). The constant c_1 in Eq. (8) has been tuned in the comparison. The two solutions found by the LHCb give very similar shapes as shown in the figure. There are a few remarks on the shapes.

(i) On the contrary with the χPT results, the parametrization in Eq. (8) does not contain the $f_0(500)$ (or the so-called σ) contribution. The LHCb Collaboration has set an upper limit for the ratio [67]:

$$R = \frac{F_r(f_0(500))}{F_r(f_0(980)} < 0.3\% \tag{12}$$

at a 90% C.L.

(ii) The expansion parameter in χPT is $p_\pi/(4\pi f_\pi)$, where the p_π is the pion's momentum. Summing higher order s-channel contributions and incorporating the coupled channel effects will extend the applicability region up to 1 GeV. However there is no guarantee that the unitarized approach is valid above 1 GeV. On the other hand, the parametrization in Eq. (8) has explicitly included two scalar resonances, $f_0(1500)$ and $f_0(1790)$, and thus is valid in the region above 1 GeV. But since in the process we are considering the dominant contributions arise from $f_0(980)$, both approaches will give similar predictions.

(iii) At the $f_0(980)$, the unitarized χPT leads to a very narrow peak. This feature is smeared out in the data since the binned results for the $\pi\pi$ invariant mass distributions are presented on the experimental side. Still the parametrization in Eq. (8) is well consistent with the data on the $B_s \to J/\psi\pi^+\pi^-$ [66,67].

(iv) From the comparison, we can see that at the current stage the advantages in both cases are not overwhelming. In the future, we hope the results can be improved in some more sophisticated methods like the unitarized approach with resonances [85]. In the following, we will use the parametrization form inspired by the data in Eq. (8).

B. Generalized LCDAs

With the scalar form factor as the normalization condition, the S-wave $\pi^+\pi^-$ LCDAs are defined by [12,98–101]

$$\begin{aligned}
\langle(\pi^+\pi^-)_S|\bar{s}(x)\gamma_\mu s(0)|0\rangle &= F^s_{\pi\pi}(m^2_{\pi\pi})p_{\pi\pi,\mu}\int_0^1 du e^{iup_{\pi\pi}\cdot x}\phi_{\pi\pi}(u),\\
\langle(\pi^+\pi^-)_S|\bar{s}(x)s(0)|0\rangle &= F^s_{\pi\pi}(m^2_{\pi\pi})B_0\int_0^1 du e^{iup_{\pi\pi}\cdot x}\phi^s_{\pi\pi}(u),\\
\langle(\pi^+\pi^-)_S\bar{s}(x)\sigma_{\mu\nu}s(0)|0\rangle &= -F^s_{\pi\pi}(m^2_{\pi\pi})B_0\frac{1}{6}(p_{\pi\pi\mu}x_\nu - p_{\pi\pi\nu}x_\mu)\\
&\quad\times\int_0^1 du e^{iup_{\pi\pi}\cdot x}\phi^\sigma_{\pi\pi}(u).
\end{aligned} \tag{13}$$

The LCDA $\phi_{\pi\pi}$ is twist-2, and the other two are twist-3. Their normalizations are given as

$$\int_0^1 du\phi^s_{\pi\pi}(u) = \int_0^1 du\phi^\sigma_{\pi\pi}(u) = 1. \tag{14}$$

The conformal symmetry in QCD [102] indicates that the twist-3 LCDA have the asymptotic form [98–101]

$$\phi^s_{\pi\pi}(u) = 1, \qquad \phi^\sigma_{\pi\pi}(u) = 6u(1-u), \tag{15}$$

while the twist-2 LCDA can be expanded in terms of the Gegenbauer moments:

$$\phi_{\pi\pi}(u) = 6u(1-u)\sum_n a_n C_n^{3/2}(2u-1). \tag{16}$$

In most cases, contributions from higher Gegenbauer moments are suppressed and thus one may keep the lowest moment a_1. It is worthwhile to stress that these LCDAs for a two-hadron system have the same form as the ones for a light scalar $\bar{q}q$ meson [98–101]. In Ref. [103], the first Gegenbauer moment for the $f_0(980)$ is calculated as[1]

$$a_1 = -1.35 \tag{17}$$

while the perturbative QCD analysis of the B_s decays has used a much smaller value [74]:

[1]In Ref. [103], the normalization factor for a scalar $\bar{q}q$ meson is $m_{f_0(980)}f_{f_0(980)}$, which is the $F^s_{\pi\pi}B_0$ in this work. The results for the twist-2 Gegenbauer moment in Eqs. (17) and (18) have been converted to our convention.

$$a_1 = -0.36. \tag{18}$$

III. HEAVY-TO-LIGHT FORM FACTORS

The $B_s \to \pi^+\pi^-$ transition can be parametrized by three form factors

$$\begin{aligned}
&\langle (\pi^+\pi^-)_S|\bar{s}\gamma_\mu\gamma_5 b|\bar{B}_s\rangle \\
&\quad = \frac{-i}{m_{B_s}}\left\{\left[P_\mu - \frac{m^2_{B_s}-m^2_{\pi\pi}}{q^2}q_\mu\right]\mathcal{F}_1^{B_s\to\pi\pi}(m^2_{\pi\pi},q^2)\right. \\
&\qquad \left. + \frac{m^2_{B_s}-m^2_{\pi\pi}}{q^2}q_\mu\mathcal{F}_0^{B_s\to\pi\pi}(m^2_{\pi\pi},q^2)\right\}, \\
&\langle (\pi^+\pi^-)_S|\bar{s}\sigma_{\mu\nu}q^\nu\gamma_5 b|\bar{B}_s\rangle \\
&\quad = \frac{\mathcal{F}_T^{B_s\to\pi\pi}(m^2_{\pi\pi},q^2)}{m_{B_s}(m_{B_s}+m_{\pi\pi})}[(m^2_{B_s}-m^2_{\pi\pi})q_\mu - q^2 P_\mu],
\end{aligned} \tag{19}$$

where the orbital angular momentum in the $\pi^+\pi^-$ system is chosen as zero in order to select the S-wave. The p_{B_s} and $p_{\pi\pi}$ is the momentum for the B_s and the $\pi\pi$ system, respectively. The momentum transfer is defined as $q = p_{B_s} - p_{\pi\pi}$, and the P_μ is defined as $P_\mu = p_{B_s} + p_{\pi\pi}$. Here the convention slightly differs with the ones adopted in Refs. [12–14]. The $D_s \to \pi^+\pi^-$ form factors can be analogously defined, with the replacement $m_{B_s} \to m_{D_s}$.

Before an explicit calculation of heavy-to-light form factors, we will discuss the impact from the complex structure of scalar mesons. The substructure of the internal scalar mesons is known to be very complex and particularly suffers from the underlying mixings among quark-antiquark states, four-quark states and other states [29–33]. As many people proposed in the literature [34–60], weak decays of heavy mesons are of great value at this point. We consider the kinematics region where the final hadron moves fast. In the large mass limit, decay amplitudes may be factorized into a short-distance hard-scattering kernel and long-distance amplitudes. To the best of our knowledge, there is no first-principle method to study long-distance amplitudes (matrix elements of the scalar meson state and QCD vacuum sandwiched by two-quark, four-quark or gluon operators). Since the mixing between different components occurs nonperturbatively, it might be plausible to assume that all long-distance matrix elements are sizable.

At a short distance, the weak transition current can be systematically expanded in $1/m_Q$ and $1/E$, where E is the large energy of the final state. Comprehensive discussions on transition form factors, in an effective field theory like soft-collinear effective theory [104–107] or perturbative QCD approach [108–111], can be found in Refs. [112–114]. Here we only quote the main phenomenology results. In the transition, the most important contributions arise from the case with the least hard scatterings. For semileptonic B_s decays into $f_0(980)$, the leading-order contributions correspond to the configuration that the $\bar{s}s$ and $\mathcal{A}_\perp\mathcal{A}_\perp$ are generated at a short distance. Here the $\mathcal{A}_\perp$ is the gluon field operator projected onto the transverse direction. Producing additional quark or gluon fields at short distance causes suppressions in terms of powers of Λ/m_Q. An estimate of the gluon contributions indicate that such contributions are less important [37,38,115,116], and in the following we will only consider the $\bar{s}s$ contribution.

It is necessary to stress that keeping only the form factor in Eq. (5) does not mean only the $\bar{s}s$ component of the internal scalar meson is probed. Instead through the power counting of the hard-scattering kernel, one observes at leading order only $\bar{s}s$ is generated at a short distance. Producing additional quark or gluon fields at short distance causes suppressions in terms of powers of Λ/m_Q. Actually the matrix element on the left-hand side Eq. (5) is a nonperturbative matrix element. Though the local operator is $\bar{s}s$, it can have nonzero overlap with other components like four-quark component through the nonperturbative QCD interactions.

As we have demonstrated in Ref. [12], at leading order the LCSR allows us to express the $B_s \to \pi^+\pi^-$ form factors in terms of the $\pi^+\pi^-$ LCDAs [98–101,117–119]. The LCSR factorization formulas read as [12]

$$\begin{aligned}
\mathcal{F}_1^{B_s\to\pi\pi}(m^2_{\pi\pi},q^2) = N_F\left\{\int_{u_0}^1\frac{du}{u}\exp\left[-\frac{m_b^2+u\bar{u}m^2_{\pi\pi}-\bar{u}q^2}{uM^2}\right]\left[-\frac{m_b}{B_0}\Phi_{\pi\pi}(u)+u\Phi^s_{\pi\pi}(u)+\frac{1}{3}\Phi^\sigma_{\pi\pi}(u)\right.\right. \\
\left.\left.+\frac{m_b^2+q^2-u^2m^2_{\pi\pi}}{uM^2}\frac{\Phi^\sigma_{\pi\pi}(u)}{6}\right]+\exp\left[-\frac{s_0}{M^2}\right]\frac{\Phi^\sigma_{\pi\pi}(u_0)}{6}\frac{m_b^2-u_0^2m^2_{\pi\pi}+q^2}{m_b^2+u_0^2m^2_{\pi\pi}-q^2}\right\},
\end{aligned} \tag{20}$$

$$\begin{aligned}
\mathcal{F}_-^{B_s\to\pi\pi}(m^2_{\pi\pi},q^2) = N_F\left\{\int_{u_0}^1\frac{du}{u}\exp\left[-\frac{m_b^2+u\bar{u}m^2_{\pi\pi}-\bar{u}q^2}{uM^2}\right]\left[\frac{m_b}{B_0}\Phi_{\pi\pi}(u)+(2-u)\Phi^s_{\pi\pi}(u)\right.\right. \\
\left.+\frac{1-u}{3u}\Phi^\sigma_{\pi\pi}(u)-\frac{u(m_b^2+q^2-u^2m^2_{\pi\pi})+2(m_b^2-q^2+u^2m^2_{\pi\pi})}{u^2M^2}\frac{\Phi^\sigma_{\pi\pi}(u)}{6}\right] \\
\left.-\frac{u_0(m_b^2+q^2-u_0^2m^2_{\pi\pi})+2(m_b^2-q^2+u_0^2m^2_{\pi\pi})}{u_0(m_b^2+u_0^2m^2_{\pi\pi}-q^2)}\exp\left[-\frac{s_0}{M^2}\right]\frac{\Phi^\sigma_{\pi\pi}(u_0)}{6}\right\},
\end{aligned} \tag{21}$$

$$\mathcal{F}_0^{B_s\to\pi\pi}(m_{\pi\pi}^2,q^2)=\mathcal{F}_1^{B_s\to\pi\pi}(m_{\pi\pi}^2,q^2)+\frac{q^2}{m_{B_s}^2-m_{\pi\pi}^2}\mathcal{F}_-^{B_s\to\pi\pi}(m_{\pi\pi}^2,q^2), \tag{22}$$

$$\mathcal{F}_T^{B_s\to\pi\pi}(m_{\pi\pi}^2,q^2)=2N_F(m_{B_s}+m_{\pi\pi})\left\{\int_{u_0}^1\frac{du}{u}\exp\left[-\frac{(m_b^2-\bar{u}q^2+u\bar{u}m_{\pi\pi}^2)}{uM^2}\right]\left[-\frac{\Phi_{\pi\pi}(u)}{2B_0}+m_b\frac{\Phi_{\pi\pi}^\sigma(u)}{6uM^2}\right]+m_b\frac{\Phi_{\pi\pi}^\sigma(u_0)}{6}\frac{\exp[-s_0/M^2]}{m_b^2-q^2+u_0^2m_{\pi\pi}^2}\right\}, \tag{23}$$

where

$$N_F=B_0F_{\pi\pi}^s(m_{\pi\pi}^2)\frac{m_b+m_s}{2m_{B_s}f_{B_s}}\exp\left[\frac{m_{B_s}^2}{M^2}\right],$$
$$u_0=\frac{m_{\pi\pi}^2+q^2-s_0+\sqrt{(m_{\pi\pi}^2+q^2-s_0)^2+4m_{\pi\pi}^2(m_b^2-q^2)}}{2m_{\pi\pi}^2}. \tag{24}$$

In order to derive the above equations, the Borel transformation of hadronic and QCD expressions of correlation functions has been carried out, defined as

$$\mathcal{B}[\mathcal{F}(Q^2)]=\lim_{Q^2\to\infty,n\to\infty,\frac{Q^2}{n}=M^2}\frac{1}{(n-1)!}(-Q^2)^n\times\left(\frac{d}{dQ^2}\right)^n\mathcal{F}(Q^2), \tag{25}$$

where $\mathcal{F}$ is a function of $Q^2=-q^2$ and M^2 is the Borel parameter. The explicit form is

$$\mathcal{B}\left[\frac{1}{(s+Q^2)^n}\right]=\frac{\exp(-s/M^2)}{(M^2)^n(n-1)!}. \tag{26}$$

This operation improves the convergence of the OPE series by factorials of n and, for suitably chosen values of M^2, enhances the contribution of the low-lying states to the correlation function.

For convenience we can define the normalized form factor:

$$\mathcal{F}_i(m_{\pi\pi}^2,q^2)=B_0F_{\pi\pi}^s(m_{\pi\pi}^2)\bar{F}_i(q^2), \tag{27}$$

where the $m_{\pi\pi}$ and q^2 dependence has been factorized into the $F_{\pi\pi}^s(m_{\pi\pi}^2)$ and $\bar{F}_i(q^2)$, respectively. This approximation is justified by the Watson-Madigal theorem [120,121]. As a reference point, we will choose the $m_{\pi\pi}=m_{f_0(980)}$ to explore the functions $\bar{F}_i(q^2)$.

In the numerical analysis, we use [33,122]

$$f_{B_s}=(224\pm5)\ \text{MeV},\qquad s_0=(34\pm2)\ \text{GeV}^2,$$
$$B_0=(1.7\pm0.2)\ \text{GeV}. \tag{28}$$

With these numerical inputs, the sum rules (20)–(23) provide us with the functions $\bar{F}_i(q^2)$ for each value of q^2 as a function of the Borel parameter. In Fig. 5, at $q^2=0$ we show the dependence on M^2 with $a_1=-0.6$. The results are obtained requiring stability against variations of M^2. As demonstrated in this figure, the form factors become stable when $M^2>12\ \text{GeV}^2$. The situations with

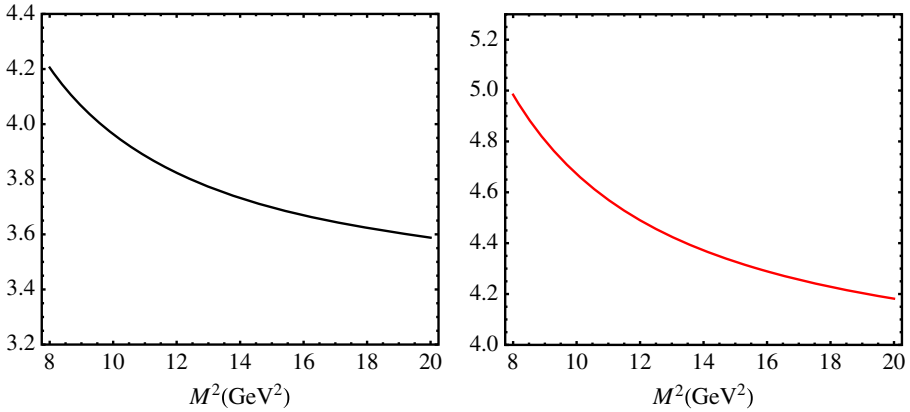

FIG. 5 (color online). At the maximal recoil $q^2=0$, the dependence of $\bar{F}_1(q^2=0)=\bar{F}_0(q^2=0)$ (left panel) and $\bar{F}_T(q^2=0)$ (right panel) on the Borel parameter M^2. The final results are obtained requiring stability against variations of M^2.

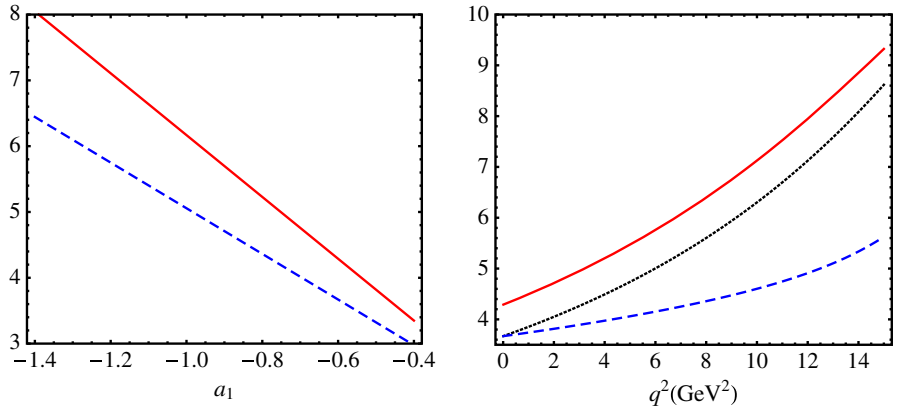

FIG. 6 (color online). At the maximal recoil $q^2 = 0$, the dependence of $\bar{F}_{1,0}$ and $\bar{F}_T$ on the Gegenbauer moment a_1 is shown in the left panel. Dashed and solid curves correspond to $\bar{F}_1(q^2 = 0) = \bar{F}_0(q^2 = 0)$, and $\bar{F}_T(q^2 = 0)$, respectively. In the right panel, the q^2 dependence is given with $a_1 = -0.6$. Solid, dotted and dashed lines denote the $\bar{F}_T(q^2)$, $\bar{F}_1(q^2)$ and $\bar{F}_0(q^2)$, respectively.

different a_1 and q^2 values are similar and thus we can choose $M^2 = (16 \pm 2)\ \mathrm{GeV}^2$.

Since the form factors are sensitive to the Gegenbauer moment a_1 of the twist-2 LCDA, in the left panel of Fig. 6 we show this dependence in the range $a_1 = (-1.4, -0.4)$ at the maximal recoil $q^2 = 0$. We will show later the value $a_1 = -0.6$ can describe well the data on both the $B_s \to \pi^+\pi^-\ell^+\ell^-$ and $D_s \to \pi^+\pi^-\ell\nu$.

The LCSR is applicable in the hard-scattering region. To access the momentum distribution in the full kinematics region, we will adopt the following parametrization

$$\bar{F}_i(q^2) = \frac{\bar{F}_i(0)}{1 - a_i q^2/m_{B_s}^2 + b_i (q^2/m_{B_s}^2)^2}, \qquad (29)$$

where $i = 1, 0, T$. The parameters can be fitted in the region $q^2 < 5\ \mathrm{GeV}^2$ for the B_s transition, and the results are collected in Table II.

For the $D_s \to \pi^+\pi^-$ transition, we use [33]

$$s_0 = (6.5 \pm 1)\ \mathrm{GeV}^2,$$
$$f_{D_s} = (257.5 \pm 4.6)\ \mathrm{MeV}, \qquad m_c = 1.4\ \mathrm{GeV}. \qquad (30)$$

The results for the $D_s \to \pi^+\pi^-$ form factors are given in Fig. 7. From the left panel, we can see the results are stable when $M^2 > 6\ \mathrm{GeV}^2$, and we will use $M^2 = (8 \pm 1)\ \mathrm{GeV}^2$. The dependence on the first Gegenbauer moment a_1 is less severe compared to the $B_s \to \pi^+\pi^-$ case, as shown in the right panel of Fig. 7. In the D_s mode, the twist-2 contributions in the regions with $x > 1/2$ and $x < 1/2$ cancel with each other. This fact has been explored in the study of $D_s \to f_0(980)$ transition [44]. Since the energy release in the D_s transition is small, we have used the $-5\ \mathrm{GeV}^2 < q^2 < 0$ to fit the q^2-dependent parameters in Eq. (29).

IV. PHENOMENOLOGICAL RESULTS

A. $B_s \to \pi^+\pi^-\ell^+\ell^-$

We proceed with the analysis of $B_s \to \pi^+\pi^-\ell^+\ell^-$, whose decay amplitude is governed by the effective Hamiltonian [123]

$$\mathcal{H}_{\mathrm{eff}} = -\frac{G_F}{\sqrt{2}} V_{tb} V_{ts}^* \sum_{i=1}^{10} C_i(\mu) O_i(\mu).$$

The O_i is a four-quark or a magnetic-moment operator, and the $C_i(\mu)$ is its Wilson coefficient. The explicit forms can be found in Ref. [123]. G_F is the Fermi constant, and $V_{tb} = 0.99914 \pm 0.00005$ and $V_{ts} = -0.0405^{+0.011}_{-0.012}$ [33] are the CKM matrix elements. The bottom and strange quark masses are $m_b = (4.66 \pm 0.03)\ \mathrm{GeV}$ and $m_s = (0.095 \pm 0.005)\ \mathrm{GeV}$ [33].

In general, various partial waves of two-hadron M_1M_2 state contribute to a generic $B \to M_1M_2\ell^+\ell^-$ process and the differential decay width has been derived using the helicity amplitude in Refs. [3–5]. In $B_s \to \pi^+\pi^-\mu^+\mu^-$, the S-wave contribution dominates with the angular distribution:

TABLE II. Fitted parameters of the $B_s/D_s \to \pi^+\pi^-$ form factors derived by LCSR.

$B_s \to \pi^+\pi^-$	$\bar{F}_i(q^2 = 0)$	a_i	b_i	$D_s \to \pi^+\pi^-$	$\bar{F}_i(q^2 = 0)$	a_i	b_i
$\bar{F}_1$	3.66	1.39	0.54	$\bar{F}_1$	2.45	0.82	0.20
$\bar{F}_0$	3.66	0.54	−0.08	$\bar{F}_0$	2.45	0.39	−0.15
$\bar{F}_T$	4.29	1.33	0.54				

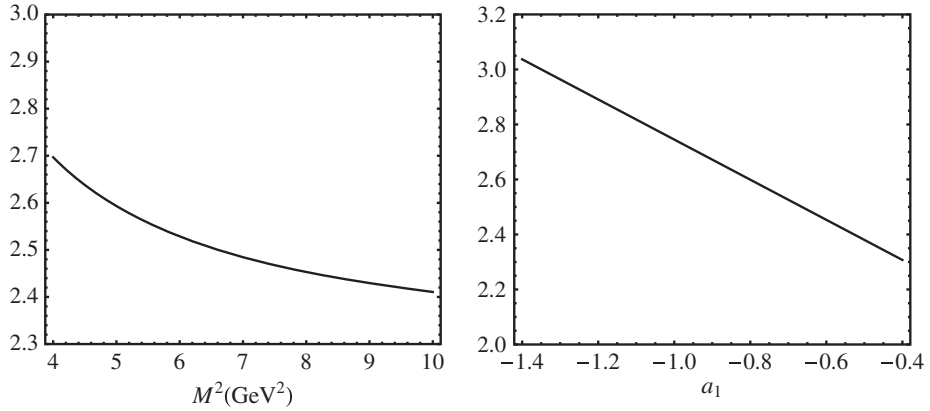

FIG. 7. The functions $\bar{F}_i(0)$ for the $D_s \to \pi^+\pi^-$: the dependence on M^2 (Gegenbauer moment a_1) in the left (right) panel.

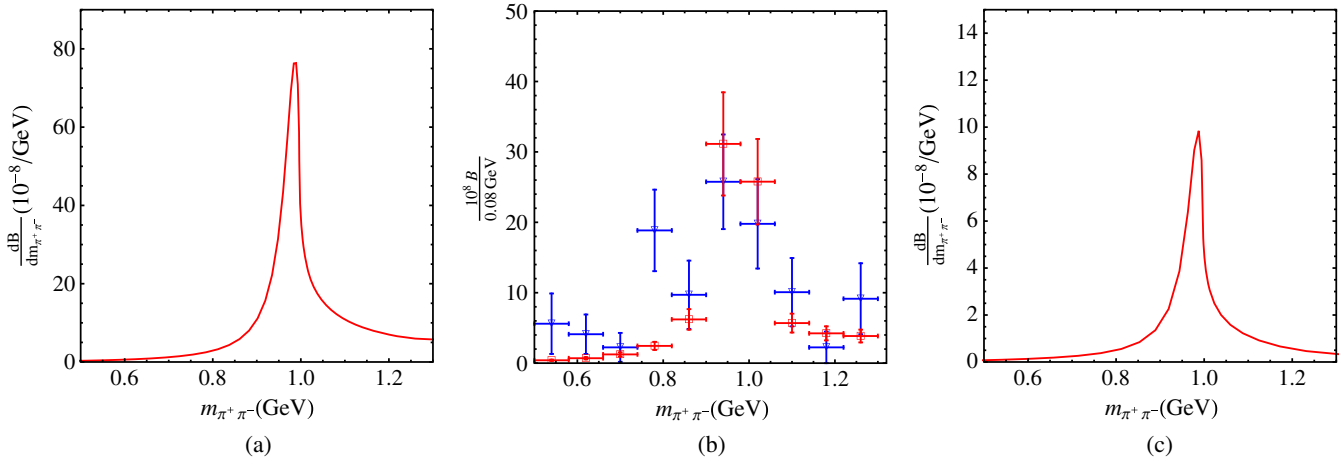

FIG. 8 (color online). Differential branching ratios $d\mathcal{B}/dm_{\pi\pi}$ for the $B_s \to \pi^+\pi^-\mu^+\mu^-$ in panels (a) and (b), and $B_s \to \pi^+\pi^-\tau^+\tau^-$ in panel (c). In panel (b), experimental data (with triangle markers) has been normalized to the central value of the branching fraction: $\mathcal{B}(B_s^0 \to \pi^+\pi^-\mu^+\mu^-) = (8.6 \pm 1.5 \pm 0.7 \pm 0.7) \times 10^{-8}$ [73], and theoretical results are shown with square markers.

$$\frac{d^3\Gamma(B_s \to \pi^+\pi^-\mu^+\mu^-)}{dm_{\pi\pi}^2 dq^2 d\cos\theta_\ell} = \frac{3}{8}[J_1^c + J_2^c \cos(2\theta_\ell)], \tag{31}$$

where the coefficients are

$$J_1^c = |\mathcal{A}_{L0}^0|^2 + |\mathcal{A}_{R0}^0|^2 + 8\hat{m}_\ell^2 |\mathcal{A}_{L0}^0 \mathcal{A}_{R0}^{0*}| \cos(\delta_{L0}^0 - \delta_{R0}^0) + 4\hat{m}_\ell^2 |\mathcal{A}_t^0|^2, \tag{32}$$

$$J_2^c = -\beta_{2\ell}^2 \{|\mathcal{A}_{L0}^0|^2 + |\mathcal{A}_{R0}^0|^2\}. \tag{33}$$

In the above equations, $\beta_{2\ell} = \sqrt{1 - 4\hat{m}_\ell^2}$, $\hat{m}_\ell = m_\ell/\sqrt{q^2}$, and θ_ℓ is the polar angle between the B_s and the μ^- moving direction in the lepton pair rest frame. The δ_{L0}^0 and δ_{R0}^0 are phases of the helicity amplitudes

$$\mathcal{A}_{L/R,0}^0 = N_1^{2\ell}\sqrt{N_2^{2\ell}}\, i \frac{1}{m_{B_s}}\left[(C_9 \mp C_{10})\frac{\sqrt{\lambda}}{\sqrt{q^2}}\mathcal{F}_1^{B_s\to\pi\pi}(q^2) + 2(C_{7L} - C_{7R})\frac{\sqrt{\lambda} m_b}{\sqrt{q^2}(m_B + m_{\pi\pi})}\mathcal{F}_T^{B_s\to\pi\pi}(q^2)\right],$$
$$\mathcal{A}_{L/R,t}^0 = N_1^{2\ell}\sqrt{N_2^{2\ell}}\, i \frac{1}{m_{B_s}}\left[(C_9 \mp C_{10})\frac{m_{B_s}^2 - m_{\pi\pi}^2}{\sqrt{q^2}}\mathcal{F}_0^{B_s\to\pi\pi}(q^2)\right], \tag{34}$$

$$\mathcal{A}_t^0 = \mathcal{A}_{R,t}^0 - \mathcal{A}_{L,t}^0 = 2N_1^{2\ell}\sqrt{N_2^{2\ell}} C_{10}\, i \frac{1}{m_{B_s}}\left[\frac{m_{B_s}^2 - m_{\pi\pi}^2}{\sqrt{q^2}}\mathcal{F}_0^{B_s\to\pi\pi}(q^2)\right], \tag{35}$$

where

$$N_1^{2\ell} = \frac{G_F}{4\sqrt{2}}\frac{\alpha_{\rm em}}{\pi} V_{tb}V_{ts}^*, \tag{36}$$

$$N_2^{2\ell} = \frac{1}{16\pi^2}\sqrt{1-4m_\pi^2/m_{\pi\pi}^2}\times\frac{8}{3}\frac{\sqrt{\lambda}q^2\beta_{2\ell}}{256\pi^3 m_{B_s}^3}. \tag{37}$$

The Källen function λ is related to the $\pi^+\pi^-$ momentum in the B_s rest frame:

$$\lambda \equiv \lambda(m_{B_s}^2, m_{\pi^+\pi^-}^2, q^2),$$
$$\lambda(a,b,c) = a^2+b^2+c^2-2(ab+bc+ca). \tag{38}$$

In Fig. 8, results for differential branching fractions $d\mathcal{B}/dm_{\pi\pi}$ for the $B_s \to \pi^+\pi^-\mu^+\mu^-$ are given in panels (a) and (b), and the ones for $B_s \to \pi^+\pi^-\tau^+\tau^-$ are given in panel (c). The result in panel (a) clearly shows the peak corresponding to the $f_0(980)$. In order to compare with the experimental data [73], we also give the binned results in panel (b) in Fig. 8 from 0.5 GeV to 1.3 GeV with square markers. Dominant theoretical errors arise from the $B_0 = (1.7 \pm 0.2)$ GeV. The experimental data (with triangle markers) has been normalized to the central value in Eq. (1). The comparison in this panel shows an overall agreement between our theoretical predictions and the experimental data. Integrating out the $m_{\pi\pi}$ from 0.5 to 1.3 GeV, we have the branching fraction

$$\mathcal{B}(B_s \to \pi^+\pi^-\mu^+\mu^-) = (6.9 \pm 1.6)\times 10^{-8}, \tag{39}$$

which is also consistent with the data in Eq. (2).

In Fig. 9, we predict the differential distribution $d\mathcal{B}/dq^2$ (in units of $10^{-8}/\text{GeV}^2$) for $B_s \to \pi^+\pi^-\mu^+\mu^-$ (solid curve) and for $B_s \to \pi^+\pi^-\tau^+\tau^-$ (dashed curve). Results for the integrated branching fractions of $B_s \to \pi^+\pi^-\tau^+\tau^-$ are predicted as

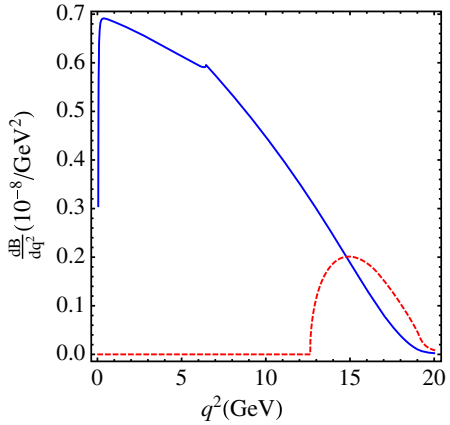

FIG. 9 (color online). The differential branching ratio $d\mathcal{B}/dq^2$ for the $B_s \to \pi^+\pi^-\mu^+\mu^-$ (solid curve) and $B_s \to \pi^+\pi^-\tau^+\tau^-$ (dashed curve) is given in units of $10^{-8}/\text{GeV}^2$.

$$\mathcal{B}(B_s \to \pi^+\pi^-\tau^+\tau^-) = (8.8 \pm 2.1)\times 10^{-9}, \tag{40}$$

where 0.5 GeV $< m_{\pi\pi} <$ 1.3 GeV is assumed. Our theoretical results could be examined at the future experimental facilities including the LHCb detector [124] and the Super-B factory at the KEK [125].

B. $B_s \to \pi^+\pi^-\nu\bar{\nu}$

The $b \to s\nu\bar{\nu}$ effective Hamiltonian is given by

$$\mathcal{H}_{b\to s\nu\bar{\nu}} = \frac{G_F}{\sqrt{2}}\frac{\alpha_{\rm em}}{2\pi\sin^2(\theta_W)} V_{tb}V_{ts}^*\eta_X X(x_t) O_L \equiv C_L O_L, \tag{41}$$

which involves the four-fermion operator

$$O_L = [\bar{s}\gamma^\mu(1-\gamma_5)b][\bar{\nu}\gamma_\mu(1-\gamma_5)\nu]. \tag{42}$$

Here θ_W is the Weinberg angle; the function $X(x_t)$ ($x_t = m_t^2/m_W^2$, with m_t the top quark mass and m_W the W mass) has been computed in Refs. [123,126], and the QCD factor η_X is found close to one [127–129].

With the above Hamiltonian, we obtain the differential decay width

$$\frac{d^2\Gamma(\bar{B}_s \to (\pi^+\pi^-)\nu\bar{\nu})}{dq^2 dm_{\pi\pi}^2} = 3\times|A_0^0|^2, \tag{43}$$

where the factor 3 arises from three species of neutrinos. The helicity amplitude in this case is

$$A_0^0 = C_L\sqrt{N_2^\nu}\, i\frac{1}{m_{B_s}}\left[\frac{\sqrt{\lambda}}{\sqrt{q^2}}\mathcal{F}_1^{B_s\to\pi\pi}(m_{\pi\pi}^2, q^2)\right],$$
$$N_2^{2\nu} = \frac{1}{16\pi^2}\sqrt{1-4m_\pi^2/m_{\pi\pi}^2}\times\frac{8}{3}\frac{\sqrt{\lambda}q^2}{256\pi^3 m_{B_s}^3}. \tag{44}$$

We give our predictions for the differential distributions for $B_s \to \pi^+\pi^-\nu\bar{\nu}$ in Fig. 10: the left panel for $d\mathcal{B}/dm_{\pi\pi}$, and the right one for $d\mathcal{B}/dq^2$. The integrated branching fraction in the range 0.5 GeV $< m_{\pi\pi} <$ 1.3 GeV is predicted as

$$\mathcal{B}(B_s \to \pi^+\pi^-\nu\bar{\nu}) = (4.9 \pm 1.2)\times 10^{-7}. \tag{45}$$

There is a large chance to measure this branching ratio at the Super-B factory at KEK [125].

C. $D_s \to \pi^+\pi^-\ell\nu$

The effective Hamiltonian for $c \to s\ell\nu$ transition is given as

$$\mathcal{H}_{c\to s\ell\nu} = N_1^\ell[\bar{s}\gamma_\mu(1-\gamma_5)c][\bar{\nu}\gamma^\mu(1-\gamma_5)\ell] + \text{H.c.}, \tag{46}$$

with

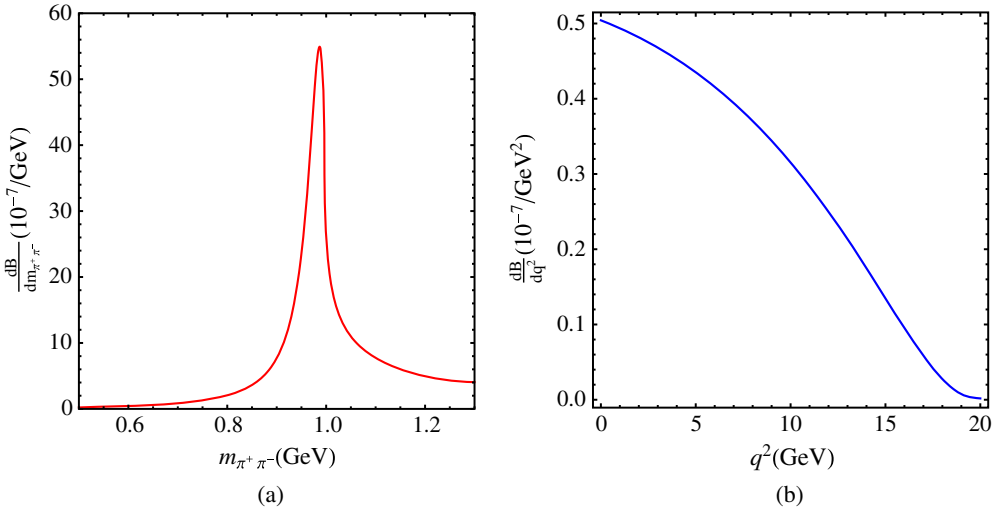

FIG. 10 (color online). The differential branching ratios for $B_s \to \pi^+\pi^-\nu\bar{\nu}$: the left panel for $d\mathcal{B}/dm_{\pi\pi}$, and the right one for $d\mathcal{B}/dq^2$.

$$N_1^{\ell} = \frac{G_F}{\sqrt{2}} V_{cs}. \tag{47}$$

The differential decay width for $D_s \to \pi^+\pi^-\ell\nu_\ell$ can be expressed as

$$\frac{d^3\Gamma}{dm_{K\pi}^2 dq^2 d\cos\theta_l} = \frac{3}{8}[I_1(q^2, m_{K\pi}^2) + I_2(q^2, m_{K\pi}^2)\cos(2\theta_l) + I_6\cos(\theta_l)], \tag{48}$$

with the I_i having the form

$$\begin{aligned} I_1(q^2, m_{\pi\pi}^2) &= [(1+\hat{m}_l^2)|A_0^0|^2 + 2\hat{m}_l^2|A_t^0|^2], \\ I_2(q^2, m_{\pi\pi}^2) &= -\beta_l|A_0^0|^2, \\ I_6(q^2, m_{\pi\pi}^2) &= 4\hat{m}_l^2 \mathrm{Re}[A_0^0 A_t^{0*}]. \end{aligned} \tag{49}$$

Using the $D_s \to \pi^+\pi^-$ form factors, the matrix element for D_s decays into the S-wave $\pi\pi$ final state is given as

$$\begin{aligned} A_0^0 &= N_1^{\ell}\sqrt{N_2^{\ell}}\, i \frac{1}{m_{D_s}}\left[\frac{\sqrt{\lambda}}{\sqrt{q^2}}\mathcal{F}_1^{D_s\to\pi\pi}(m_{\pi\pi}^2, q^2)\right], \\ A_t^0 &= N_1^{\ell}\sqrt{N_2^{\ell}}\, i \frac{1}{m_{D_s}}\left[\frac{m_{D_s}^2 - m_{\pi\pi}^2}{\sqrt{q^2}}\mathcal{F}_0^{D_s\to\pi\pi}(m_{\pi\pi}^2, q^2)\right], \end{aligned} \tag{50}$$

where

$$N_2^{\ell} = \frac{1}{16\pi^2}\sqrt{1 - 4m_\pi^2/m_{\pi\pi}^2} \times \frac{8}{3}\frac{\sqrt{\lambda}q^2\beta_\ell}{256\pi^3 m_{D_s}^3}. \tag{51}$$

As discussed in Ref. [13], one can explore a number of the q^2-dependent ratios and in particular the lepton flavor dependent ratio:

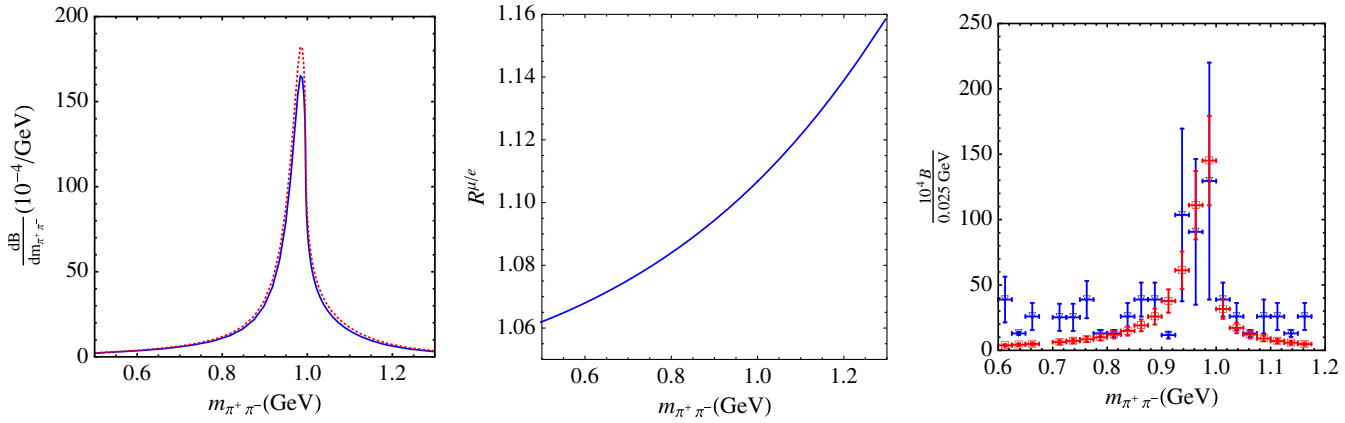

FIG. 11 (color online). The differential branching ratios for $D_s \to \pi^+\pi^-\ell\nu$. The first panel corresponds to $d\mathcal{B}/dm_{\pi\pi}$, in which the dotted and solid curves correspond to $D_s \to \pi^+\pi^-\mu\nu$ and $D_s \to \pi^+\pi^- e\nu$, respectively. The second panel shows the ratio $R^{\mu/e}(m_{\pi\pi}^2)$ defined in Eq. (53). A comparison with the experimental data [76,77] is given in panel (c).

$$\mathcal{R}^{\mu/e}(m_{\pi\pi}^2, q^2) = \frac{d^2\Gamma(D_s \to \pi^+\pi^-\mu^+\nu_\mu)/dq^2 dm_{\pi\pi}^2}{d^2\Gamma(D_s \to \pi^+\pi^-e^+\nu_e)/dq^2 dm_{\pi\pi}^2}, \quad (52)$$

and the integrated form over q^2:

$$R^{\mu/e}(m_{\pi\pi}^2) = \frac{d\Gamma(D_s \to \pi^+\pi^-\mu^+\nu_\mu)/dm_{\pi\pi}^2}{d\Gamma(D_s \to \pi^+\pi^-e^+\nu_e)/dm_{\pi\pi}^2}. \quad (53)$$

Our results are given in Fig. 11. The first panel corresponds to $d\mathcal{B}/dm_{\pi\pi}$, in which the dotted and solid curves denote $D_s \to \pi^+\pi^-\mu\nu$ and $D_s \to \pi^+\pi^-e\nu$, respectively. One different behavior in the differential branching ratio with $B_s \to \pi^+\pi^-\ell^+\ell^-$ in the $m_{\pi\pi}$ distributions is the suppression in the large $m_{\pi\pi}$ region. The second panel shows the ratio $R^{\mu/e}(m_{\pi\pi}^2)$ defined in Eq. (53). A comparison with the experimental data on the differential branching fraction [76,77] is given in panel (c), where we can also find the agreement.

The integrated branching fractions are predicted as

$$\mathcal{B}(D_s \to \pi^+\pi^-e^+\nu) = (1.52 \pm 0.36) \times 10^{-3}, \quad (54)$$

$$\mathcal{B}(D_s \to \pi^+\pi^-\mu^+\nu) = (1.68 \pm 0.39) \times 10^{-3}, \quad (55)$$

where 0.5 GeV $< m_{\pi\pi} <$ 1.3 GeV has been adopted in the integration. Again the errors come from the QCD condensate parameter B_0. Theoretical results are in good agreement with the CLEO results in Eqs. (3), (4) [76–78]. We expect experimental errors will be greatly reduced since in the future the BES-III Collaboration will collect about 2 fb^{-1} data in e^+e^- collision at the energy around 4.17 GeV which will be used to study semileptonic and nonleptonic D_s decays [79].

V. CONCLUSIONS

Rare B decays have played an important role in testing the SM, and hunting for the NP. In recent years, a lot of experimental progress has been made on $B \to K^*\ell^+\ell^-$, and remarkably the LHCb Collaboration has found a 3.7σ deviation from the SM for the ratio P_5'. This observable P_5' is believed almost independent on the hadronic uncertainties.

The analysis of $B \to V\ell^+\ell^-$, more appropriately $B \to M_1M_2\ell^+\ell^-$, requests not only the knowledge on the m_b expansion but also the M_1M_2 final state interactions. In this work, we have studied the $B_s^0 \to \pi^+\pi^-\ell^+\ell^-$, $B_s^0 \to \pi^+\pi^-\nu\bar{\nu}$ and $D_s^+ \to \pi^+\pi^-\ell^+\nu$ decay in the kinematics region where the $\pi^+\pi^-$ system has a invariant mass in the range 0.5–1.3 GeV. These processes are dominated by the S-wave contributions and thus they are valuable towards the determination of the S-wave $\pi^+\pi^-$ light-cone distribution amplitudes which are normalized to scalar form factors. We have compared the results for scalar form factors calculated in unitarized χPT and the ones extracted from the data on $B_s \to J/\psi\pi^+\pi^-$. We have derived the $B_s \to \pi^+\pi^-$ and $D_s \to \pi^+\pi^-$ transition form factor using the light-cone sum rules, and then presented our results for differential decay width which agree well with experimental data. Accurate measurements by the BES-III at the BEPC, the LHCb at the LHC and Super-B factory at KEKB in the future will be valuable to more precisely examine our formalism, and determine the two-hadron LCDA.

ACKNOWLEDGMENTS

The authors are grateful to Zhi-Hui Guo, Hsiang-Nan Li, Cai-Dian Lü, Ulf-G. Meißner, Wen-Fei Wang, and Rui-Lin Zhu for enlightening discussions. This work was supported in part by Shanghai Natural Science Foundation under Grants No. 15DZ2272100 and No. 15ZR1423100, by the Open Project Program of State Key Laboratory of Theoretical Physics, Institute of Theoretical Physics, Chinese Academy of Sciences, China (No. Y5KF111CJ1), and by the Scientific Research Foundation for the Returned Overseas Chinese Scholars, State Education Ministry, and National Natural Science Foundation of China under Grant No. 11575110.

[1] R. Aaij *et al.* (LHCb Collaboration), Measurement of Form-Factor-Independent Observables in the Decay $B^0 \to K^{*0}\mu^+\mu^-$, Phys. Rev. Lett. **111**, 191801 (2013).
[2] LHCb Collaboration, Report No. LHCb-CONF-2015-002, CERN-LHCb-CONF-2015-002.
[3] C. D. Lu and W. Wang, Analysis of $B \to K_J^*(\to K\pi)\mu^+\mu^-$ in the higher kaon resonance region, Phys. Rev. D **85**, 034014 (2012).
[4] B. Dey, Angular analyses of exclusive $\bar{B} \to X\ell_1\ell_2$ with complex helicity amplitudes, Phys. Rev. D **92**, 033013 (2015).
[5] J. Gratrex, M. Hopfer, and R. Zwicky, Generalised helicity formalism, higher moments and the $B \to K_{J_K}(\to K\pi)\bar{\ell}_1\ell_2$ angular distributions, arXiv:1506.03970.
[6] D. Becirevic and A. Tayduganov, Impact of $B \to K_0^*\ell^+\ell^-$ on the new physics search in $B \to K^*\ell^+\ell^-$ decay, Nucl. Phys. **B868**, 368 (2013).
[7] J. Matias, On the S-wave pollution of $B \to K * l + l-$ observables, Phys. Rev. D **86**, 094024 (2012).
[8] T. Blake, U. Egede, and A. Shires, The effect of S-wave interference on the $B^0 \to K^{*0}\ell^+\ell^-$ angular observables, J. High Energy Phys. 03 (2013) 027.

[9] D. Das, G. Hiller, M. Jung, and A. Shires, The $\bar{B} \to \bar{K}\pi\ell\ell$ and $\bar{B}_s \to \bar{K}K\ell\ell$ distributions at low hadronic recoil, J. High Energy Phys. 09 (2014) 109.

[10] L. Hofer and J. Matias, Exploiting the symmetries of P and S wave for $B \to K^*\mu^+\mu^-$, J. High Energy Phys. 09 (2015) 104.

[11] D. Das, G. Hiller, and M. Jung, $B \to K\pi\ell\ell$ in and outside the K^* window, arXiv:1506.06699.

[12] U. G. Meißner and W. Wang, Generalized heavy-to-light form factors in light-cone sum rules, Phys. Lett. B **730**, 336 (2014).

[13] U. G. Meißner and W. Wang, $B_s \to K^{(*)}\ell\bar{\nu}$, angular analysis, S-wave contributions and $|\mathbf{V_{ub}}|$, J. High Energy Phys. 01 (2014) 107.

[14] M. Dring, U. G. Meißner, and W. Wang, Chiral dynamics and S-wave contributions in semileptonic B decays, J. High Energy Phys. 10 (2013) 011.

[15] W. Wang, Recent developments on the CKM matrix, Int. J. Mod. Phys. A **29**, 1430040 (2014).

[16] S. Gardner and U. G. Meißner, Rescattering and chiral dynamics in $B \to \rho\pi$ decay, Phys. Rev. D **65**, 094004 (2002).

[17] M. Maul, Semileptonic B decays and the two pion distribution amplitudes, Eur. Phys. J. C **21**, 115 (2001).

[18] X. W. Kang, B. Kubis, C. Hanhart, and U. G. Meißner, B_{l4} decays and the extraction of $|V_{ub}|$, Phys. Rev. D **89**, 053015 (2014).

[19] W. H. Liang and E. Oset, B^0 and B_s^0 decays into $J/\psi f_0(980)$ and $J/\psi f_0(500)$ and the nature of the scalar resonances, Phys. Lett. B **737**, 70 (2014).

[20] M. Bayar, W. H. Liang, and E. Oset, B^0 and B_s^0 decays into J/ψ plus a scalar or vector meson, Phys. Rev. D **90**, 114004 (2014).

[21] J. J. Xie and E. Oset, $\bar{B}^0$ and $\bar{B}_s^0$ decays into J/ψ and $f_0(1370), f_0(1710), f_2(1270), f_2'(1525), K_2^*(1430)$, Phys. Rev. D **90**, 094006 (2014).

[22] M. Sayahi and H. Mehraban, Final state interaction in $B^0 \to J/\psi\ \pi^+\pi^-$ decay, Phys. Scr. **88**, 035101 (2013).

[23] T. Sekihara and E. Oset, Investigating the nature of light scalar mesons with semileptonic decays of D mesons, Phys. Rev. D **92**, 054038 (2015).

[24] L. Roca, M. Mai, E. Oset, and U. G. Meißner, Predictions for the $\Lambda_b \to J/\psi\Lambda(1405)$ decay, Eur. Phys. J. C **75**, 218 (2015).

[25] C. H. Chen and H. n. Li, Three body nonleptonic B decays in perturbative QCD, Phys. Lett. B **561**, 258 (2003).

[26] C. H. Chen and H. n. Li, Vector pseudoscalar two meson distribution amplitudes in three body B meson decays, Phys. Rev. D **70**, 054006 (2004).

[27] W.-F. Wang, H.-C. Hu, H.-n. Li, and C.-D. Lü, Direct CP asymmetries of three-body B decays in perturbative QCD, Phys. Rev. D **89**, 074031 (2014).

[28] H. s. Wang, S. m. Liu, J. Cao, X. Liu, and Z. j. Xiao, The three body decays $B^+ \to \pi^+\pi^-\pi^+$ in perturbative QCD approach, Nucl. Phys. **A930**, 117 (2014).

[29] S. Godfrey and J. Napolitano, Light meson spectroscopy, Rev. Mod. Phys. **71**, 1411 (1999).

[30] F. E. Close and N. A. Tornqvist, Scalar mesons above and below 1 GeV, J. Phys. G **28**, R249 (2002).

[31] E. Klempt and A. Zaitsev, Glueballs, hybrids, multiquarks: Experimental facts versus QCD inspired concepts, Phys. Rep. **454**, 1 (2007).

[32] A. H. Fariborz, R. Jora, and J. Schechter, Global aspects of the scalar meson puzzle, Phys. Rev. D **79**, 074014 (2009).

[33] K. A. Olive *et al.* (Particle Data Group Collaboration), Review of particle physics, Chin. Phys. C **38**, 090001 (2014).

[34] J. L. Rosner, Scalar mesons in charm decays, AIP Conf. Proc. **1030**, 30 (2008).

[35] W. Wang, Y. L. Shen, Y. Li, and C.-D. Lü, Study of scalar mesons $f_0(980)$ and $f_0(1500)$ from $B \to f_0(980)K$ and $B \to f_0(1500)K$ decays, Phys. Rev. D **74**, 114010 (2006).

[36] Y. L. Shen, W. Wang, J. Zhu, and C.-D. Lü, Study of $K_0^*(1430)$ and $a_0(980)$ from $B \to K_0^*(1430)\pi$ and $B \to a_0(980)K$ decays, Eur. Phys. J. C **50**, 877 (2007).

[37] W. Wang, Y. L. Shen, and C.-D. Lü, B-to-glueball form factor and glueball production in B decays, J. Phys. G **37**, 085006 (2010).

[38] W. F. Wang, Y. Y. Fan, M. Liu, and Z. J. Xiao, Semileptonic decays $B/B_s \to (\eta, \eta', G)(l^+l^-, l\bar{\nu}, \nu\bar{\nu})$ in the perturbative QCD approach beyond the leading order, Phys. Rev. D **87**, 097501 (2013).

[39] Y. M. Wang, M. J. Aslam, and C.-D. Lü, Scalar mesons in weak semileptonic decays of $B_{(s)}$, Phys. Rev. D **78**, 014006 (2008).

[40] B. El-Bennich, O. Leitner, J.-P. Dedonder, and B. Loiseau, The scalar meson $f_0(980)$ in heavy-meson decays, Phys. Rev. D **79**, 076004 (2009).

[41] N. Ghahramany and R. Khosravi, Analysis of the rare semileptonic decays of B_s to $f_0(980)$ and K_0^*, (1430) scalar mesons in QCD sum rules, Phys. Rev. D **80**, 016009 (2009).

[42] C. S. Kim, Y. Li, and W. Wang, Study of decay modes $B \to K_{(0)}^*(1430)\phi$, Phys. Rev. D **81**, 074014 (2010).

[43] W. Wang and C.-D. Lü, Distinguishing two kinds of scalar mesons from heavy meson decays, Phys. Rev. D **82**, 034016 (2010).

[44] P. Colangelo, F. De Fazio, and W. Wang, $B_s \to f_0(980)$ form factors and B_s decays into $f_0(980)$, Phys. Rev. D **81**, 074001 (2010).

[45] O. Leitner, J.-P. Dedonder, B. Loiseau, and B. El-Bennich, Scalar resonance effects on the $B_{(s)} - \bar{B}_{(s)}$ mixing angle, Phys. Rev. D **82**, 076006 (2010).

[46] X. Liu and Z. J. Xiao, Light scalar mesons and charmless hadronic $B_c \to SP, SV$ decays in the perturbative QCD approach, Phys. Rev. D **82**, 054029 (2010).

[47] Y. J. Sun, Z. H. Li, and T. Huang, $B_{(s)} \to S$ transitions in the light cone sum rules with the chiral current, Phys. Rev. D **83**, 025024 (2011).

[48] C. D. L, U. G. Meißner, W. Wang, and Q. Zhao, Hunting for a scalar glueball in exclusive B decays, Eur. Phys. J. A **49**, 58 (2013).

[49] R. Fleischer, R. Knegjens, and G. Ricciardi, Anatomy of $B_{s,d}^0 \to J/\psi f_0(980)$, Eur. Phys. J. C **71**, 1832 (2011).

[50] A. H. Fariborz, R. Jora, J. Schechter, and M. N. Shahid, Probing pseudoscalar and scalar mesons in semileptonic decays of D_s^+, D^+ and D^0, Int. J. Mod. Phys. A **30**, 1550012 (2015).

[51] S. Stone and L. Zhang, Use of $B \to J/\psi f_0$ Decays to Discern the $q\bar{q}$ or Tetraquark Nature of Scalar Mesons, Phys. Rev. Lett. **111**, 062001 (2013).

[52] Y. K. Hsiao, C. C. Lih, and C. Q. Geng, Semileptonic $B^- \to f_0(1710, 1500, 1370)e^-\bar{\nu}_e$ decays, Phys. Rev. D **89**, 077501 (2014).

[53] R. Dutta and S. Gardner, CP asymmetries in $B \to f_{(0)}K_{(S)}$ decays, Phys. Rev. D **78**, 034021 (2008).

[54] D. Delepine, J. L. Lucio M., J. A. Mendoza S., and C. A. Ramirez, A consistent scenario for $B \to PS$ decays, Phys. Rev. D **78**, 114016 (2008).

[55] R. H. Li, C. D. Lu, W. Wang, and X. X. Wang, $B \to S$ transition form factors in the PQCD approach, Phys. Rev. D **79**, 014013 (2009).

[56] Z. Q. Zhang and Z. J. Xiao, $B \to f_{(0)}(980)(\pi, \eta')$ decays in the PQCD approach, Chin. Phys. C **33**, 508 (2009).

[57] Z. Q. Zhang and Z. J. Xiao, Study of scalar meson $a_{(0)}(980)$ from $B \to a_{(0)}(980)\pi$ decays, Chin. Phys. C **34**, 528 (2010).

[58] Z. Q. Zhang, Study of scalar meson $f_0(980)$ and $K_0^*(1430)$ from $B \to f_0(980)\rho(\omega, \phi)$ and $B \to K_0^*(1430)\rho(\omega)$ decays, Phys. Rev. D **82**, 034036 (2010).

[59] J. W. Li, D. S. Du, and C.-D. Lü, Determination of $f_0 - \sigma$ mixing angle through $B_s^0 \to J/\Psi f_0(980)(\sigma)$ decays, Eur. Phys. J. C **72**, 2229 (2012).

[60] P. Colangelo, F. De Fazio, and W. Wang, Nonleptonic B_s to charmonium decays: Analyses in pursuit of determining the weak phase β_s, Phys. Rev. D **83**, 094027 (2011).

[61] S. Stone and L. Zhang, S-waves and the measurement of CP violating phases in B_s decays, Phys. Rev. D **79**, 074024 (2009).

[62] S. Stone and L. Zhang, Measuring the CP violating phase in B_s mixing using $B_s^0 \to J/\psi f_{(0)}(980)$, arXiv:0909.5442.

[63] R. Aaij *et al.* (LHCb Collaboration), First observation of $B_s^0 \to J/\psi f_0(980)$ decays, Phys. Lett. B **698**, 115 (2011).

[64] R. Aaij *et al.* (LHCb Collaboration), Measurement of the CP violating phase ϕ_s in $\bar{B}_s^0 \to J/\psi f_0(980)$, Phys. Lett. B **707**, 497 (2012).

[65] R. Aaij *et al.* (LHCb Collaboration), Analysis of the resonant components in $\bar{B}_s^0 \to J/\psi\pi^+\pi^-$, Phys. Rev. D **86**, 052006 (2012).

[66] R. Aaij *et al.* (LHCb Collaboration), Analysis of the resonant components in $\bar{B}_0 \to J/\psi\pi^+\pi^-$, Phys. Rev. D **87**, 052001 (2013).

[67] R. Aaij *et al.* (LHCb Collaboration), Measurement of resonant and CP components in $\bar{B}_s^0 \to J/\psi\pi^+\pi^-$ decays, Phys. Rev. D **89**, 092006 (2014).

[68] R. Aaij *et al.* (LHCb Collaboration), Measurement of the resonant and CP components in $\bar{B}^0 \to J/\psi\pi^+\pi^-$ decays, Phys. Rev. D **90**, 012003 (2014).

[69] J. Li *et al.* (Belle Collaboration), Observation of $B_s^0 \to J/\psi f_0(980)$ and Evidence for $B_s^0 \to J/\psi f_0(1370)$, Phys. Rev. Lett. **106**, 121802 (2011).

[70] T. Aaltonen *et al.* (CDF Collaboration), Measurement of branching ratio and B_s^0 lifetime in the decay $B_s^0 \to J/\psi f_0(980)$ at CDF, Phys. Rev. D **84**, 052012 (2011).

[71] V. M. Abazov *et al.* (D0 Collaboration), Measurement of the relative branching ratio of $B_s^0 \to J/\psi f_0(980) \to B_s^0 \to J/\psi\phi$, Phys. Rev. D **85**, 011103 (2012).

[72] F. E. Close and A. Kirk, Interpretation of scalar and axial mesons in LHCb from a historical perspective, Phys. Rev. D **91**, 114015 (2015).

[73] R. Aaij *et al.* (LHCb Collaboration), Study of the rare B_s^0 and B^0 decays into the $\pi^+\pi^-\mu^+\mu^-$ final state, Phys. Lett. B **743**, 46 (2015).

[74] W. F. Wang, H. n. Li, W. Wang, and C.-D. Lü, S-wave resonance contributions to the $B_{(s)}^0 \to J/\psi\pi^+\pi^-$ and $B_s \to \pi^+\pi^-\mu^+\mu^-$ decays, Phys. Rev. D **91**, 094024 (2015).

[75] W. Wang and R. L. Zhu, To understand the rare decay, $B_s \to \pi^+\pi^-\ell^+\ell^-$, Phys. Lett. B **743**, 467 (2015).

[76] J. Yelton *et al.* (CLEO Collaboration), Absolute branching fraction measurements for exclusive $D_{(s)}$ semileptonic decays, Phys. Rev. D **80**, 052007 (2009).

[77] K. M. Ecklund *et al.* (CLEO Collaboration), Study of the semileptonic decay $D_{(s)}^+ \to f_0(980)e^+\nu$ and implications for $B_{(s)} \to J/\psi f_{(0)}$, Phys. Rev. D **80**, 052009 (2009).

[78] J. Hietala, D. Cronin-Hennessy, T. Pedlar, and I. Shipsey, Exclusive D_s semileptonic branching fraction measurements, Phys. Rev. D **92**, 012009 (2015).

[79] D. M. Asner *et al.*, Physics at BES-III, Int. J. Mod. Phys. A **24**, 499 (2009).

[80] P. Colangelo and A. Khodjamirian, QCD sum rules, a modern perspective, arXiv:hep-ph/0010175.

[81] J. Gasser and U. G. Meißner, Chiral expansion of pion form factors beyond one loop, Nucl. Phys. **B357**, 90 (1991).

[82] U. G. Meißner and J. A. Oller, $J/\psi \to \phi\pi\pi$ (K anti-K) decays, chiral dynamics and OZI violation, Nucl. Phys. **A679**, 671 (2001).

[83] J. Bijnens and P. Talavera, $K_{(l3)}$ decays in chiral perturbation theory, Nucl. Phys. **B669**, 341 (2003).

[84] T. A. Lahde and U. G. Meißner, Improved analysis of J/ψ decays into a vector meson and two pseudoscalars, Phys. Rev. D **74**, 034021 (2006).

[85] Z. H. Guo, J. A. Oller, and J. Ruiz de Elvira, Chiral dynamics in form factors, spectral-function sum rules, meson-meson scattering and semi-local duality, Phys. Rev. D **86**, 054006 (2012).

[86] J. Gasser and H. Leutwyler, Chiral perturbation theory to one loop, Ann. Phys. (N.Y.) **158**, 142 (1984).

[87] J. Gasser and H. Leutwyler, Chiral perturbation theory: Expansions in the mass of the strange quark, Nucl. Phys. **B250**, 465 (1985).

[88] J. Gasser and H. Leutwyler, Low-energy expansion of meson form factors, Nucl. Phys. **B250**, 517 (1985).

[89] J. F. Donoghue, J. Gasser, and H. Leutwyler, The decay of a light Higgs boson, Nucl. Phys. **B343**, 341 (1990).

[90] J. A. Oller, E. Oset, and J. R. Pelaez, Meson meson interaction in a nonperturbative chiral approach, Phys. Rev. D **59**, 074001 (1999); **60**, 099906(E) (1999); **75**, 099903(E) (2007).

[91] J. A. Oller and E. Oset, N/D description of two meson amplitudes and chiral symmetry, Phys. Rev. D **60**, 074023 (1999).

[92] D. Jido, J. A. Oller, E. Oset, A. Ramos, and U. G. Meissner, Chiral dynamics of the two $\Lambda(1405)$ states, Nucl. Phys. **A725**, 181 (2003).

[93] J. A. Oller, E. Oset, and A. Ramos, Chiral unitary approach to meson-meson and meson-baryon interactions and nuclear applications, Prog. Part. Nucl. Phys. **45**, 157 (2000).
[94] A. Gomez Nicola and J. R. Pelaez, Meson meson scattering within one loop chiral perturbation theory and its unitarization, Phys. Rev. D **65**, 054009 (2002).
[95] M. Ablikim *et al.* (BES Collaboration), Resonances in $J/\psi \to \phi\pi^+\pi^-$ and ϕK^+K^-, Phys. Lett. B **607**, 243 (2005).
[96] S. M. Flatte, Coupled-channel analysis of the $\pi\eta$ and K anti-K systems near K anti-K threshold, Phys. Lett. **63B**, 224 (1976).
[97] S. M. Flatte, On the nature of 0^+ mesons, Phys. Lett. **63B**, 228 (1976).
[98] M. Diehl, T. Gousset, B. Pire, and O. Teryaev, Probing Partonic Structure in $\gamma^*\gamma \to \pi\pi$ near Threshold, Phys. Rev. Lett. **81**, 1782 (1998).
[99] M. V. Polyakov, Hard exclusive electroproduction of two pions and their resonances, Nucl. Phys. **B555**, 231 (1999).
[100] N. Kivel, L. Mankiewicz, and M. V. Polyakov, NLO corrections and contribution of a tensor gluon operator to the process $\gamma^*\gamma \to \pi\pi$, Phys. Lett. B **467**, 263 (1999).
[101] M. Diehl, Generalized parton distributions, Phys. Rep. **388**, 41 (2003).
[102] V. M. Braun, G. P. Korchemsky, and D. Mueller, The uses of conformal symmetry in QCDm, Prog. Part. Nucl. Phys. **51**, 311 (2003).
[103] H. Y. Cheng, C. K. Chua, and K. C. Yang, Charmless hadronic B decays involving scalar mesons: Implications to the nature of light scalar mesons, Phys. Rev. D **73**, 014017 (2006).
[104] C. W. Bauer, S. Fleming, and M. E. Luke, Summing Sudakov logarithms in $B \to X(s\gamma)$ in effective field theory, Phys. Rev. D **63**, 014006 (2000).
[105] C. W. Bauer, S. Fleming, D. Pirjol, and I. W. Stewart, An effective field theory for collinear and soft gluons: Heavy to light decays, Phys. Rev. D **63**, 114020 (2001).
[106] C. W. Bauer, D. Pirjol, and I. W. Stewart, Soft collinear factorization in effective field theory, Phys. Rev. D **65**, 054022 (2002).
[107] M. Beneke and T. Feldmann, Factorization of heavy-to-light form factors in soft-collinear effective theory, Nucl. Phys. **B685**, 249 (2004).
[108] Y.-Y. Keum, H.-N. Li, and A. I. Sanda, Fat penguins and imaginary penguins in perturbative QCD, Phys. Lett. B **504**, 6 (2001).
[109] Y. Y. Keum, H.-N. Li, and A. I. Sanda, Penguin enhancement and $B \to K\pi$ decays in perturbative QCD, Phys. Rev. D **63**, 054008 (2001).
[110] C.-D. Lü, K. Ukai, and M.-Z. Yang, Branching ratio and CP violation of $B \to \pi\pi$ decays in perturbative QCD approach, Phys. Rev. D **63**, 074009 (2001).
[111] C.-D. Lä and M.-Z. Yang, $B \to \pi\rho$, $\pi\omega$ decays in perturbative QCD approach, Eur. Phys. J. C **23**, 275 (2002).
[112] M. Beneke and T. Feldmann, Symmetry breaking corrections to heavy to light B meson form factors at large recoil, Nucl. Phys. **B592**, 3 (2001).
[113] C. W. Bauer, D. Pirjol, and I. W. Stewart, Factorization and endpoint singularities in heavy to light decays, Phys. Rev. D **67**, 071502 (2003).
[114] T. Kurimoto, H.-N. Li, and A. I. Sanda, Leading power contributions to $B \to \pi, \rho$ transition form factors, Phys. Rev. D **65**, 014007 (2001).
[115] A. R. Williamson and J. Zupan, Two body B decays with isosinglet final states in SCET, Phys. Rev. D **74**, 014003 (2006); **74**, 039901(E) (2006).
[116] W. Wang, Y. M. Wang, D. S. Yang, and C. D. Lu, Charmless two-body $B_{(s)} \to VP$ decays in soft collinear effective theory, Phys. Rev. D **78**, 034011 (2008).
[117] D. Müller, D. Robaschik, B. Geyer, F.-M. Dittes, and J. Hořejši, Wave functions, evolution equations and evolution kernels from light ray operators of QCD, Fortschr. Phys. **42**, 101 (1994).
[118] P. Hagler, B. Pire, L. Szymanowski, and O. V. Teryaev, Hunting the QCD odderon in hard diffractive electroproduction of two pions, Phys. Lett. B **535**, 117 (2002); **540**, 324(E) (2002).
[119] B. Pire, F. Schwennsen, L. Szymanowski, and S. Wallon, Hard Pomeron-Odderon interference effects in the production of $\pi^+\pi^-$ pairs in high energy $\gamma\gamma$ collisions at the LHC, Phys. Rev. D **78**, 094009 (2008).
[120] K. M. Watson, The effect of final state interactions on reaction cross sections, Phys. Rev. **88**, 1163 (1952).
[121] A. B. Migdal, The theory of nuclear reactions with production of slow particles, Sov. Phys. JETP **1**, 2 (1955).
[122] S. Aoki *et al.*, Review of lattice results concerning low-energy particle physics, Eur. Phys. J. C **74**, 2890 (2014).
[123] G. Buchalla, A. J. Buras, and M. E. Lautenbacher, Weak decays beyond leading logarithms, Rev. Mod. Phys. **68**, 1125 (1996).
[124] R. Aaij *et al.* (LHCb Collaboration), Implications of LHCb measurements and future prospects, Eur. Phys. J. C **73**, 2373 (2013).
[125] T. Aushev *et al.*, Physics at Super B Factory, arXiv:1002.5012.
[126] T. Inami and C. S. Lim, Effects of superheavy quarks and leptons in low-energy weak processes $K_{(L)} \to \mu\bar{\mu}$, $K^+ \to \pi^+\nu\bar{\nu}$ and $K^0 \leftrightarrow \bar{K}^0$, Prog. Theor. Phys. **65**, 297 (1981); **65**, 1772(E) (1981).
[127] G. Buchalla and A. J. Buras, QCD corrections to rare K and B decays for arbitrary top quark mass, Nucl. Phys. **B400**, 225 (1993).
[128] G. Buchalla and A. J. Buras, The rare decays $K \to \pi\nu\bar{\nu}$, $B \to X\nu\bar{\nu}$ and $B \to l^+l^-$: An update, Nucl. Phys. **B548**, 309 (1999).
[129] M. Misiak and J. Urban, QCD corrections to FCNC decays mediated by Z penguins and W boxes, Phys. Lett. B **451**, 161 (1999).